

## Article

# Preparation, Antimicrobial Activity and Docking Study of Vanadium Mixed Ligand Complexes Containing 4-Amino-5-hydrazinyl-4*H*-1,2,4-triazole-3-thiol and Aminophenol Derivatives

Doaa Domyati <sup>1</sup>, Sami A. Zabin <sup>2</sup>, Ahmed A. Elhenawy <sup>2,3</sup>  and Mohamed Abdelbaset <sup>2,4,\*</sup>

<sup>1</sup> Department of Chemistry, College of Science, University of Jeddah, Jeddah 21589, Saudi Arabia; Dmdomyati@uj.edu.sa

<sup>2</sup> Chemistry Department, Faculty of Science, Albaha University, Abaha 65731, Saudi Arabia; szabin@bu.edu.sa (S.A.Z.); ahmed.elhenawy@azhar.edu.eg (A.A.E.)

<sup>3</sup> Chemistry Department, Faculty of Science, Al-Azhar University, Cairo 11884, Egypt

<sup>4</sup> Chemistry Department, Faculty of Science, Al-Azhar University, Assiut Branch, Assiut 71524, Egypt

\* Correspondence: baset1002002@yahoo.co.uk



**Citation:** Domyati, D.; Zabin, S.A.; Elhenawy, A.A.; Abdelbaset, M. Preparation, Antimicrobial Activity and Docking Study of Vanadium Mixed Ligand Complexes Containing 4-Amino-5-hydrazinyl-4*H*-1,2,4-triazole-3-thiol and Aminophenol Derivatives. *Processes* **2021**, *9*, 1008. <https://doi.org/10.3390/pr9061008>

Academic Editors: Yunfei Du, Kang Hyun Park and Andrea Melchior

Received: 6 April 2021

Accepted: 4 June 2021

Published: 7 June 2021

**Publisher's Note:** MDPI stays neutral with regard to jurisdictional claims in published maps and institutional affiliations.



**Copyright:** © 2021 by the authors. Licensee MDPI, Basel, Switzerland. This article is an open access article distributed under the terms and conditions of the Creative Commons Attribution (CC BY) license (<https://creativecommons.org/licenses/by/4.0/>).

**Abstract:** The synthesis of mixed-ligand complexes is considered an important strategy for developing new metal complexes of enhanced biological activity. This paper presents the synthesis, characterization, in vitro antimicrobial assessment, and theoretical molecular docking evaluation for synthesized oxidovanadium (V) complexes. The proposed structures of the synthesized compounds were proved using elemental and different spectroscopic analysis. The antimicrobial tests showed moderate activity of the compounds against the Gram-positive bacterial strains and the fungal yeast, whereas no activity was observed against the Gram-negative bacterial strains. The performance of density functional theory (DFT) was conducted to study the interaction mode of the targeted compounds with the biological system. Calculating the quantitative structure-activity relationship (QSPR) was performed depending on optimization geometries, frontier molecular orbitals (FMOs), and chemical reactivities for synthesized compounds. The molecular electrostatic potentials (MEPs) that were plotted link the interaction manner of synthesized compounds with the receptor. The molecular docking evaluation revealed that the examined compounds may possess potential antibacterial activity.

**Keywords:** 1,2,4-triazole-3-thiol; vanadium (V) complexes; in silico pharmacokinetic; antimicrobial activity; molecular docking

## 1. Introduction

Compounds having a 1,2,4-triazole ring-system represent an interesting class of heterocyclic compounds and are the focus of many researchers due to their ease of synthesis and their application diversity, especially as therapeutic agents [1–4]. These compounds have interesting physical properties such as solubility, dipole character, and hydrogen bonding capacity; they act as important pharmacophores due to their interacting ability with biological receptors [5]. Additionally, molecules with 1,2,4-triazole moiety along with some adjacent donor groups are potential ligands used for designing interesting coordination compounds with interesting applications [6]. Molecules with 1,2,4-triazole moiety are very strong N-atom donors towards d-metal ions and can be readily deprotonated [7]. There is more focus on developing metal complexes as promising potential therapeutic agents because researchers believe that the coordination of organic molecules with metal ions enhances their biological activity [8–11].

Vanadium coordination compounds are one of these compounds that have attracted the interest of many research due to their involvement in several biological processes and as they are also known as prospective inhibitors of various enzymes [12,13].

Oxidovanadium (IV and V) complexes have been reported to exhibit insulin-mimetic activity, cell differentiation stimulatory and inhibitory actions, anti-microbial activity, tumor growth inhibition, and prophylaxis against carcinogenesis [14]. Moreover, vanadium and its compounds inhibit several ATPases, different phosphatases, and some enzymes like ribonucleases, phosphodiesterases, and glucose-6-phosphatase [14].

Moreover, it is reported that Oxidovanadium (IV) and dioxidovanadium (V) complexes exhibit comparable or larger anti-mycobacterium tuberculosis activities than the free parent organic ligands [15].

The literature survey revealed that the strategy of designing metal complexes with mixed ligands is a promising approach for developing new compounds bearing better biological activity [16]. Complexes designed through combining ligands with biological activity and metals having therapeutic potential proved to have enhanced biological activity [11,12,16]. Vanadium mixed ligands complexes were reported as medicinal agents for treating different diseases [15].

Keeping in view the significant bioactive nature of the ligand molecules with triazoles nucleus as well as vanadium complexes, the present work aimed to synthesize vanadium (V) mixed-ligand complexes involving the heterocyclic 4-amino-5-hydrazinyl-4H-1,2,4-triazole-3-thiol as primary ligand and aminophenol derivatives as secondary ligands. To evaluate the biological activities of the tested vanadium complexes, the docking calculations were run to investigate the possibility of an interaction between these compounds and DNA gyrase. This protein was selected due to their reported studies [17,18], which revealed that these complexes can bind to the DNA gyrase and could be considered as biologically active compound [19]. Additionally, the synthesized complexes were screened *in vitro* for antimicrobial activity and were subjected to theoretical molecular docking evaluation [20–23].

## 2. Materials and Methods

### 2.1. Materials and Physical Measurements

The chemicals used in experimentation were purchased from Sigma-Aldrich (St. Louis, MO, USA) and used as received. Melting points of the prepared compounds were determined using Electrothermal (Cat NO. TA9100) melting point apparatus. Molar conductivities of freshly prepared dimethyl formamide (DMF) solutions of the complexes at a concentration of 0.001M were measured using Hanna instrument HI8633N Multi-range conductivity meter.

### 2.2. Elemental Analysis and Spectroscopy

Elemental analysis for C, H, N, and S were carried out using Leco VTF-900 CHN-S-O 932 version 1.3× (ThermoFisher Scientific, Waltham, MA, USA) instrument. FT-IR spectra were recorded on Nicolet IS50 FT-IR spectrophotometer in the range of 400–4000  $\text{cm}^{-1}$ . UV-visible spectra for the complexes in DMF solvent were recorded on Evolution 300 UV-vis Spectrophotometer. Mass spectra were recorded on a Thermo Fisher Exactive + Triversa Nanomate mass spectrometer. The  $^1\text{H}$ NMR spectra were obtained using Varian Mercury-400BB (400 MHz) spectrometer using TMS (1 H) as standard.

### 2.3. Preparation of Mixed-Ligand Oxidovanadium (V) Complexes

The targeted complexes were prepared using 1:1:1 ( $L_1:M:L_{2-4}$ ) molar ratio. To a mixture of hot ethanolic solution of 4-amino-5-hydrazinyl-4H-1,2,4-triazole-3-thiol ( $L_1$ ) (0.01 mol) and *o*-phenylenediamine ( $L_2$ ), or 2-aminophenol ( $L_3$ ), or 2-aminothiophenol ( $L_4$ ) (0.01 mol), an aqueous hot solution of ammonium metavanadate ( $\text{NH}_4\text{VO}_3$ ) or potassium metavanadate ( $\text{KVO}_3$ ) (0.01 mol) was added slowly dropwise with continuous stirring and refluxing for 4 h. The complexes precipitated out from the solution were filtered washed with proper solvents and dried in open air. The purity of the compounds were checked

with TLC paper where one spot was observed confirming the formation of single complex. All the synthesized complexes were colored solid powders with reasonable yield and melting points above 300 °C.

#### 2.4. Computational Study

##### 2.4.1. Preparation of Ligands and Protein

From protein data bank RCSB, the 3D structure of protein files was downloaded for (ID: 4uro [24]) DNA Gyrase B and (ID: 1VJY [25]) transforming growth factor beta receptor type I (TGFBRI). In order to mining data of proteins we used BLAST P tool for analysis of FASTA sequence of proteins. Then, CLUSTALW package was utilized for multiple of amino acids alignments as reported earlier [26–30].

All the Quantum chemical computations for (L1, L2 & 1–6) were performed, using the DFT theory [31] with the Becke3-Lee-Yang-parr (B3LYP) level using 6-311<sup>++</sup>G(d,p) basis. The optimization Geometry for molecular structures was carried out to improve knowledge of chemical structures.

The (1-6) were built then energy minimized based on DFT/VMP [31]. The Docking process were completed by MOE 2015 package [32]. The error correction for structure of catalytic sites were performed by supplemented hydrogens and partial charges using (Amber12: EHT), then minimized by utilizing the same force field with RMSD = 0.100. The catalytic site was identified and analyzed using Site Finder program that based on alpha spheres as well as energy model [33]. The catalytic zone was predicted by the MOE-Site finder [33].

##### 2.4.2. Stepwise Docking Experiment

The Docking computations were completed by MOE 2015 package (Molecular Operating Environment (MOE)) [32]. The error correction for structure of catalytic sites into DNA Gyrase B (ID: 4uro) were performed by supplemented hydrogens and partial charges using (Amber12: EHT), then minimized through utilizing the same force field with RMSD = 0.100. The catalytic site was identified and analyzed using Site Finder program method, which is based on alpha spheres as well as energy model. The catalytic zone was predicted using the MOE-Site finder. Water and inhibitors molecules were eliminated, then H-atoms were supplemented to the obtained crystal structure. The charges were designed using MMFF94x force field. The alpha-site spheres were added depending on site-finder module. Afterwards the ligand was subjected to induced fit docking (IFD) for generating energy poses and assigning final binding scores.

#### 2.5. Assessment of Antimicrobial Capacity

The synthesized compounds were assessed against *Staphylococcus aureus* (ATCC 25923), *Streptococcus pneumoniae* (ATCC 49619) as Gram-positive bacteria strains, *Escherichia coli* (ATCC 25922), *Pseudomonas aeruginosa* (ATCC 27853) Gram-negative bacteria strains, and *Candida albicans* (ATCC 10231) as yeast. The reported Disc Diffusion Assay (DDA) method was used as assessment methodology using Muller–Hinton agar as a microbiological growth medium [33]. The stock solution of the compounds was prepared by dissolving 0.02 g of each compound in 5 mL dimethylformamide (DMF) solvent. After the incubation period, the microbial susceptibility was measured by noting the zones (in mm) of complete inhibition around each hole. Each experiment was repeated three times and results were recorded as mean value.

### 3. Results

#### 3.1. Synthesis of Oxidovanadium (V) Mixed Ligand Complexes

The designed oxidovanadium (V) mixed ligand complexes were prepared successfully using 4-amino-5-mercapto-3-phenyl-1,2,4-triazole (L<sub>1</sub>) as primary ligand and o-aniline derivatives (L<sub>2</sub>–L<sub>4</sub>) as secondary ligands mixed with the vanadium salts in 1:1:1 stoichiometric ratio ((L<sub>1</sub>:M:L<sub>2-4</sub>)). The yields obtained were in reasonable yield with a range of

70–85%. The elemental analysis obtained (Table S1, Supplementary Material) were in agreement with the proposed structure. The isolated solid compounds were dark-colored powders with high melting points ( $>300\text{ }^{\circ}\text{C}$ ) and were soluble in dimethyl formamide (DMF) and dimethyl sulfoxide (DMSO).

### 3.2. Molar Conductivity

The measured molar conductivity values (Table S1, Supplementary Material) for the prepared complexes with a concentration of  $1 \times 10^{-3}\text{ M}$  in DMSO solution at room temperature lie in the range ( $75\text{--}110.5\text{ ohm}^{-1}\text{ cm}^2\text{ mole}^{-1}$ ) indicating an electrolytic behavior and of ionic nature [34,35].

### 3.3. IR Spectra

The important infrared frequencies exhibited by the ligand ( $L_1$ ) and the obtained vanadium (V) complexes are listed in (Table S2 Supplementary Material). The ligand's ( $L_1$ ) IR spectra showed characteristic absorption bands at  $3270$ ,  $3200\text{ cm}^{-1}$  assigned for  $\text{NH}_2$  group, and  $2910\text{ cm}^{-1}$  specified for SH group. In the IR spectra of the metal complexes, it was observed that  $\text{NH}_2$  group bands were shifted their position indicating binding of  $\text{NH}_2$  group with the vanadium metal ion. The characteristic band for  $\nu(\text{SH})$  was not shown in the spectra of the vanadium (V) complexes suggested deprotonation and hence binding to the vanadium ion through S-atom [36,37].

The participation of oxygen, sulfur, and nitrogen in coordination with the metal ion is further supported by the new band appearance at  $450\text{--}480$ ,  $530\text{--}550$ , and  $590\text{--}595\text{ cm}^{-1}$  assigned for  $\nu(\text{V-S})$ ,  $\nu(\text{V-N})$ , and  $\nu(\text{V-O})$ , respectively [28,32]. In the IR spectra of some complexes a strong band and in some others medium band appeared in the range  $1440\text{--}1460\text{ cm}^{-1}$  which are due to the deformation modes of the  $\delta(\text{NH}_4^+)$  ion [37,38]. The presence of sharp band in the spectra of the vanadium complexes at  $920\text{--}980$  can be assigned to  $(\text{V}=\text{O})$  stretches [34,37]. A broad band at  $3050\text{--}3405\text{ cm}^{-1}$  was observed in the spectra of the metal complexes, which is an indication for the presence of hydrated water in the complexes [39].

These observations suggesting that the obtained vanadium complexes have the general formula  $[\text{VO}(\text{NNS})(\text{OX})]$  where  $X = \text{N, O or S}$ . The primary ligand ( $L_1$ ) coordinates to the oxidovanadium (V) center in a tridentate (NNS) fashion while, the secondary ligands ( $L_2$ ,  $L_3$ , and  $L_4$ ) coordinates to the oxidovanadium (V) center in Bidentate (NN), (NO), or (NS) [16].

### 3.4. UV-Visible Spectra

The electronic spectra of the vanadium (V) complexes in  $10^{-3}\text{ M}$  DMSO solution at room temperature (Figure S2, Supplementary Material) showed peaks at the range of  $349\text{--}356\text{ nm}$ , which may be due to the intra-ligand charge transfer  $\pi \rightarrow \pi^*$  and  $n \rightarrow \pi^*$  transitions, and other peaks in the range of  $424\text{--}440\text{ nm}$ , which are assigned to ligand-to-metal charge transfer (LMCT) transitions from the  $P^\pi$  orbital on the nitrogen, oxygen, and sulfur atoms to the empty orbital of the  $d^0$  vanadium centers [40–42].

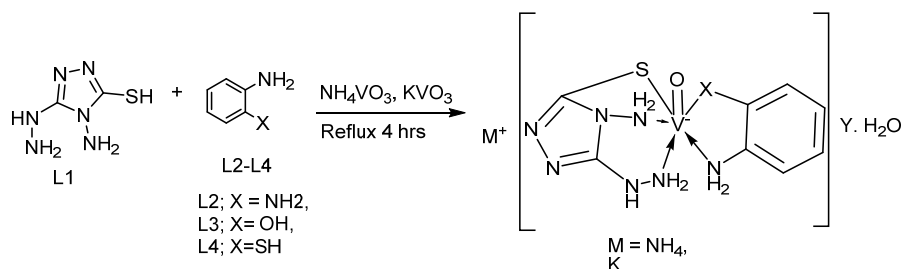
### 3.5. $^1\text{H-NMR}$ Spectra

$^1\text{H-NMR}$  spectra of the ligands and their vanadium (V) complexes (Figure S3, Supplementary Material) have been recorded in  $\text{DMSO-d}_6$  using tetramethyl silance (TMS) as internal standard. The  $^1\text{H NMR}$  spectra of the ligand ( $L_1$ ) showed the  $-\text{SH}$  proton at  $10.18\text{ ppm}$ , which was disappeared in the spectrum of the vanadium (V) complexes indicating deprotonation and coordination through the thiol group with the vanadium metal ion [43]. Furthermore, in the  $^1\text{H NMR}$  Spectra the signals of  $\text{NH}_2$  protons appear at  $\delta 5.14\text{ ppm}$ , shifted to high field in the spectra of the vanadium (V) complexes indicating bonding through the nitrogen atom of the amine group to the central vanadium ion [44]. In  $^1\text{H-NMR}$  spectrum of the vanadium (V) complexes did not show any signal in the region

12.00–12.37 suggesting deprotonation of OH group (in co-ligand L<sub>3</sub>) and coordinating to the vanadium metal ion via oxygen atom [45].

### 3.6. Mass Spectra

The mass spectra were recorded in order to confirm the theoretically calculated molecular weight according to the proposed structure (Figure S4, Supplementary Material). The observed peak for the complex NH<sub>4</sub>[VO(L<sub>1</sub>)(L<sub>2</sub>)] 2.5H<sub>2</sub>O(1) at 383.00 matches the theoretically calculated molecular weight of (383.3). The mass spectrum for K[VO(L<sub>1</sub>)(L<sub>2</sub>)] 1.5H<sub>2</sub>O (2) showed a peak at 386.58 equivalent to the calculated M. Wt. (386.35). In case of the complex NH<sub>4</sub>[VO(L<sub>1</sub>)(L<sub>3</sub>)] 4H<sub>2</sub>O(3) the observed peak at 410.08 is equivalent to the calculated M. Wt. (409.29). The observed peak for NH<sub>4</sub>[VO(L<sub>1</sub>)(L<sub>4</sub>)] H<sub>2</sub>O (5) at 372.25 matches the calculated its M. Wt. (372.32), Finally for the complex K[VO(L<sub>1</sub>)(L<sub>4</sub>)] 2H<sub>2</sub>O (6) the observed peak was at 410.17 matches the theoretical M. Wt. (411.39). These observations are in agreement with the proposed structures as shown in Scheme 1.



**Scheme 1.** Proposed structure of the M[VO(L<sub>2</sub>)(L<sub>2-4</sub>)] yH<sub>2</sub>O complexes.

### 3.7. Molecular Modeling Studies

To get clear view of the chemical structure of the complexes, the optimization geometry was achieved using density functional theory DFT/B3LYP/6-311G++(d,p) basis set level implemented in materialstudio2017 workspace. The bond length and angle for complexes were summarized in (Table S3, Supplementary Material). The optimization geometry for all tested ligands (1–6) showed that the triazoles were stabilized in parallel mode with phenyl ring, and at the same time the triazoles arranged in perpendicularity position with metal core centers (Figure S5).

The frontier molecular orbitals FMOs is circular orbitals, which include both vital orbitals (i) HOMO, highest occupied molecular orbital; and (ii) LUMO, lowest unoccupied molecular orbital. These orbitals can judge the interaction rout of the reactant species with others. FMOs gap was characterized by the chemical reactivity and kinetic stability of the molecule. The molecule possesses promising value of EHOMO and has good ability to awarding electron, as well as easier for losing electron of valence to biological media, and hence enhancing interactions with a receptor, and vice versa [46,47]. (HOMOs)/(LUMOs) have been figured in (Figure 1) for the (1–6) complexes systems in the S0 states. Figure 1 indicates the distribution of molecular orbits over studied systems. The HOMO orbital was distributed around phenyl rings for compounds 1 and 6. The complexes 2–5 were stabilized by distributing HOMO orbitals between triazoles and phenyl rings. The LUMO orbital has been covered in triazole and metal cores in all tested complexes, except V complex 6 the LUMO cloud covered only upon metal ring. From HOMO and LUMO maps the electron cloud transfer from HOMO to LUMO zones, which means there is an intramolecular electron flow from phenyl ring to metal and triazole rings in the investigated complexes. All complexes showed good stability due to high stability of the energy gap.

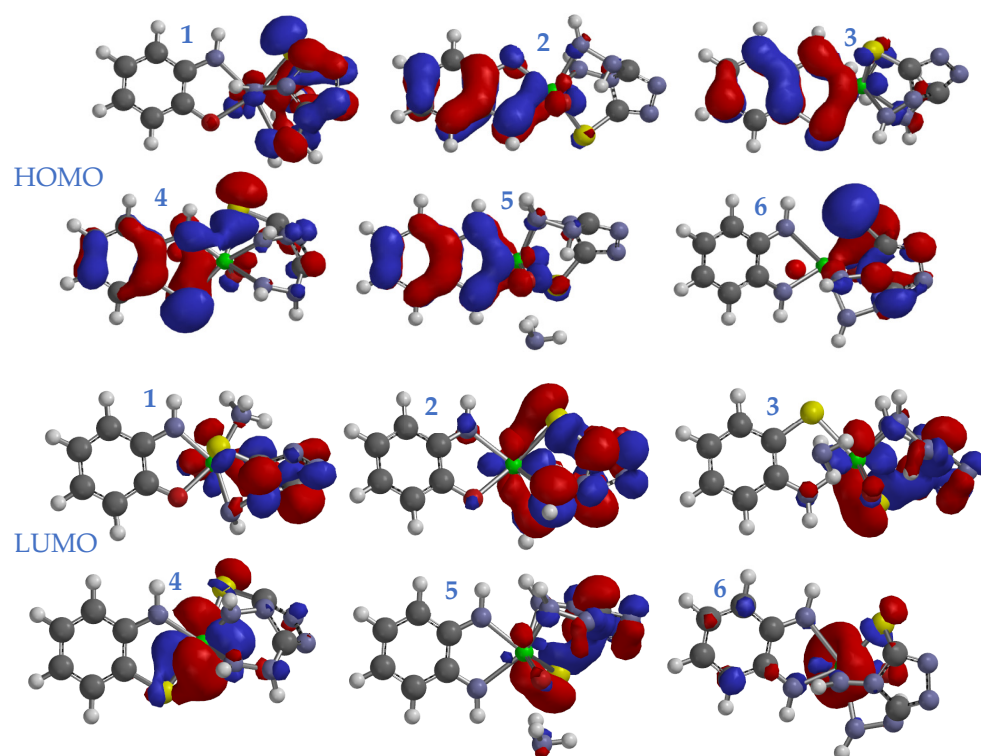


**Figure 1.** The HOMO and LUMO for complexes (1–6) at DFT theory based in B3LYP/6-311G++(d,p).

The voltage for the electrostatic map (EV) of complexes 1–6 is represented in Figure 2. From the comparison of the EV of the complexes, it can be concluded that there is distribution of positive charges around the triazole rings in all complexes 1–6 (shown in yellow to green color). The electron density, as shown in red color, is delocalized all over the skeleton of the molecular structure of the complexes 1–6. The metal core centers, having a large bond order, has a high ability of attracting electrons, and hence the increasing electron density over the metal cores. Therefore, these complexes (1–6) showed high electrophilic capacity in the biological media [48].

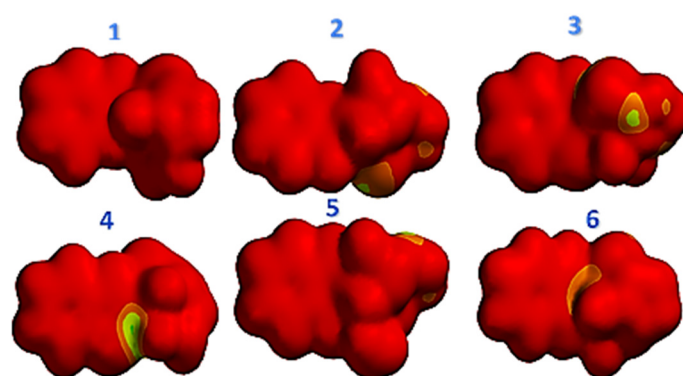


**Figure 2.** Electrostatic surface Voltage (VP) for complexes 1–6 at DFT/B3LYP/6-311G++(d,p) molecular orbital calculations, yellow colors representing -ve regions, and blue colors indicating positive regions.

### 3.8. Docking Studies

The docking study targeted (ID: 4uro) DNA Gyrase B *Candida albicans* lanosterol 14- $\alpha$ -demethylase, and (ID: 1VJY) was performed to examine the potential mode of the complexes (1–6) as antimicrobial agents. The fingerprint for ligand–protein–interactions were estimated based on the docking score through implementing function in the Molecular

Operating Environment MOE 2015.10 package (Figures 3 and 4; Figure S6, Supplementary Materials). All calculated energies of the docking simulation via crystal-structures (PDB: 4uro and 1VJy) have been summarized in (Table S4, Supplementary Material). Bacterial DNA-gyrase plays a vital role in the activity of the antibacterial agents, and acts by breaking double-stranded DNA through catalyzing negative supercoiling, which is essential for DNA replication, transcription, and recombination [49]. Analysis of the co-crystallized DNA-gyrase cleavage complex with novobiocin, which is an effective antibacterial agent that acts by cleaving DNA and restricting the ATPase binding site located on the vital peptidoglycan of the bacterial cell wall (Ser 55, Ala64, Asn.65, Asp89, Thr164, Thr173, and Val79). The inhibitory effect may be a result of the distinct structure of the cell wall that characterizes the Gram-negative and Gram-positive bacteria. The cell wall of the Gram-negative bacteria is composed of a thin peptidoglycan layer (7–8 nm) with an additional outer membrane. While the Gram-positive bacteria contain a thick peptidoglycan layer (20–80 nm) outside the cell wall with no outer membrane. The peptidoglycan is a mesh-like polymer consisting of sugars and amino acids. A peptidoglycan layer protects microorganisms against antibacterial agents such as antibiotics, toxins, chemicals, and degradative enzymes [48,50]. In addition, the crystal structure of TGF of  $\beta$ -RI bound with naphthyridine (ligand 460) was obtained as PDB file (ID: 1VJY) with 2.0Å resolution.

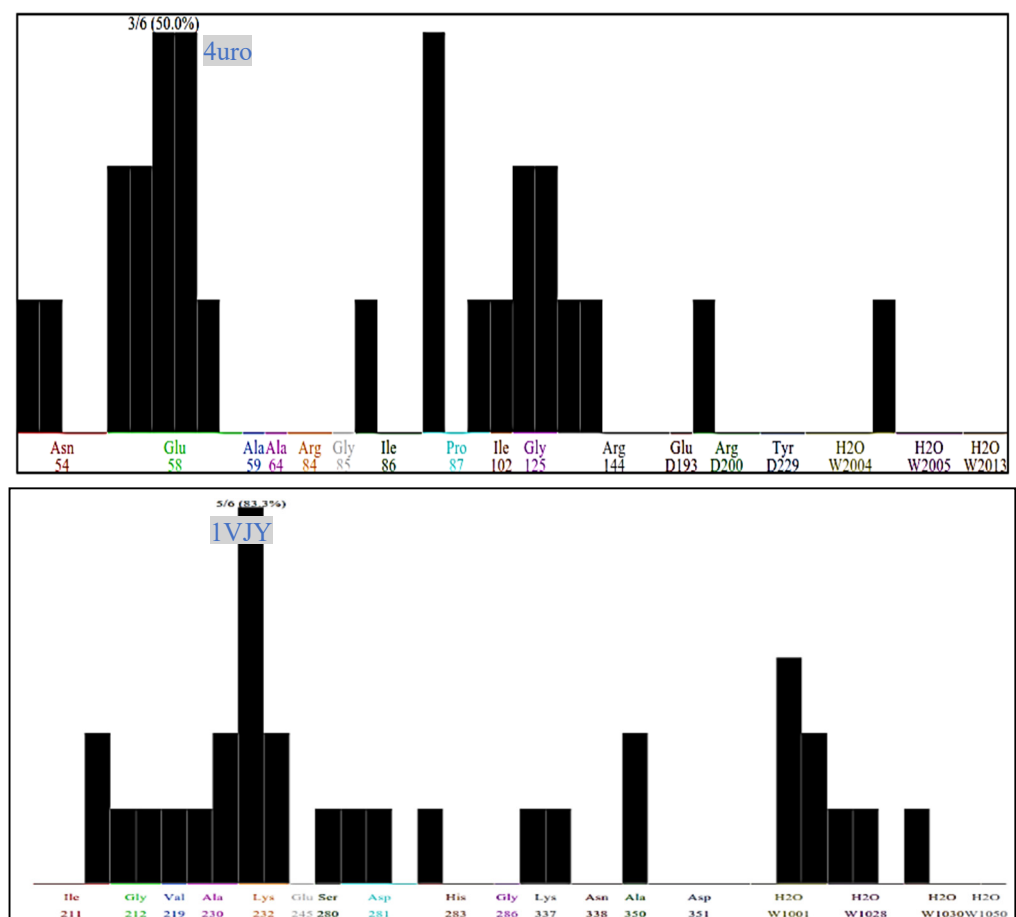


**Figure 3.** Plotted PLIF histogram which represented the interacted docked complexes 1–6 with residues of 4uro and 1VJY.

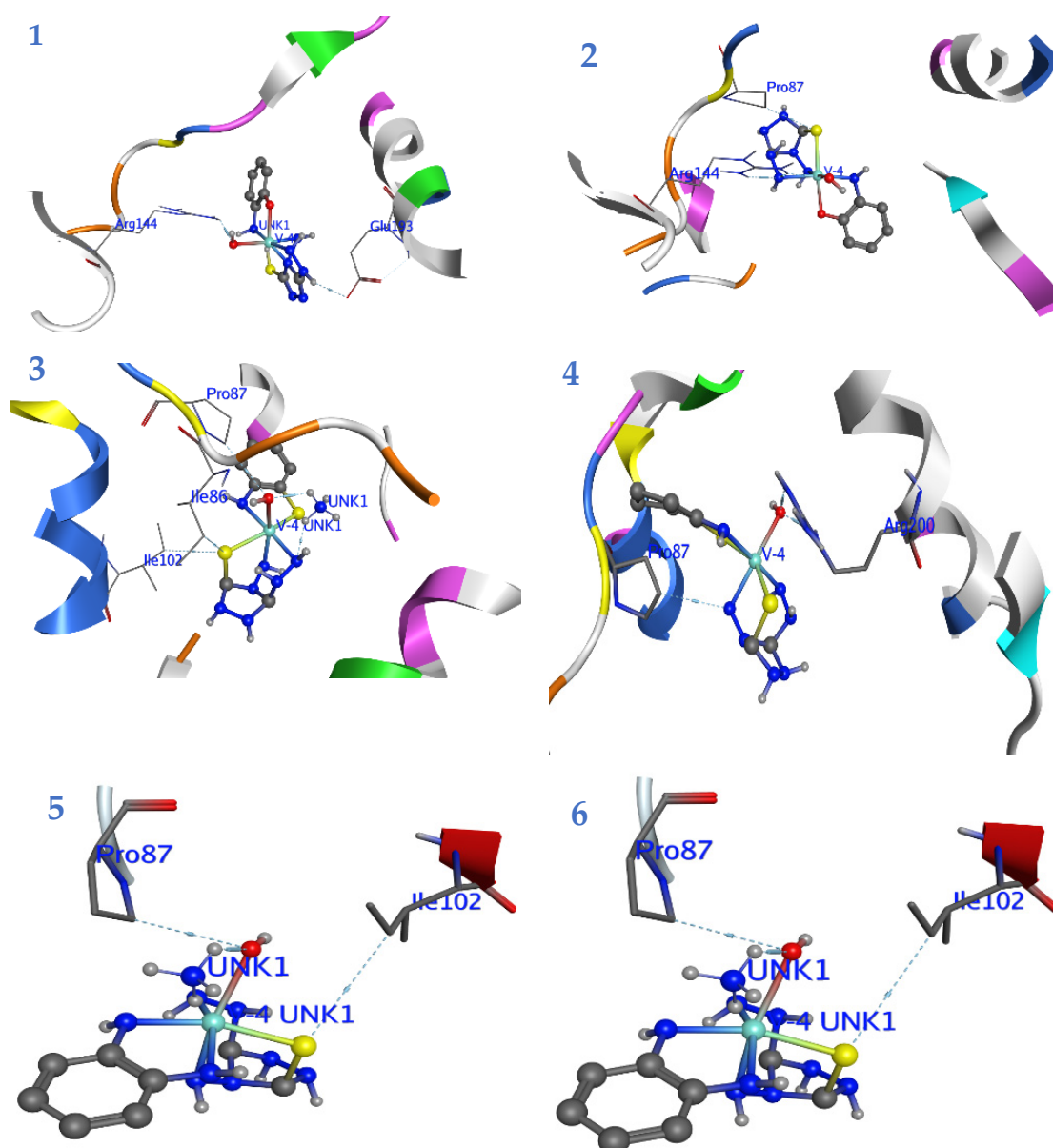


**Figure 4.** The binding mode of complexes (1–6) into the active site of DNA Gyrase, H-bond represented as blue dashed color.

The updated redocked technique has been used for 1–6 complexes into active sites in the absence of the reference inhibitor. The 1–6 complexes were successfully capped into active zone of the enzymes. The docked poses of complexes were obtained and used for energy-minimized by a molecular-mechanics (Amber12: EHT) force field, until reached 0.05/kcal/mol of the gradient convergence. The poses were filtered depending on the lowest binding free energy calculation  $\Delta G$  with the lowest root means quart deviation (RMSD) between the pose before and after refinement. The  $\Delta G$  utilized the AMBER force field combined with GB/VI solvation parameters, which considered the contributions of the solvation in binding process [51]. Finally, the highest MOE scoring function for the tested compounds was applied to evaluate the binding affinities of the tested compounds (Table S4, Supplementary Material).

**(ID: 4uro) DNA Gyrase B:** The complex 1 exhibited the highest binding affinity (−4.4 Kcal/mol.) compared with other 2–6 complexes. The other 2–6 complexes showed nearly the same considerable binding potency as well as RMSD. The scores of the binding energy were arranged as  $3 > 4 > 2 > 5 > 6$  with a trend for  $\Delta G$  between  $\sim -3.9$  and  $-3.01$  (Table S4, Supplementary Material). All compounds allowed H-bond formation with important amino acid residues (Glu.58, Pro.87, Ile.102, and Gly.125) at the DNA gyrase active site (Figure S6, Supplementary Materials). The analysis of the protein ligand fingerprint PLIF-consensus was graphed in Figure 3. Interestingly, PLIF showed the Glu.58 and pro.87 are combined with 50% of tested complexes.

All compounds were arranged in perpendicular mode with Pro.87 and Glu.58 (see Figure 4). The hydrophobic residues and presence of ammonia and potassium in the outer shell of complexes 1–6 played a stabilization factor for the receptors-conformation. The variation in the complexes-conformations sensed the interactions with the hydrophilic amino acid backbone at the 4uro binding site (Figure S6, Supplementary Materials).

From the above data, one can deduced that the hydrophobic residues of complexes played a circular pharmabiotic for binding to the DNA-gyrase pocket. Furthermore, the inhibition potency of 1–6 complexes for bacterial growth may be due to the attacking-power against the peptidoglycan-naked cell-wall of bacteria [52,53]. Thus, the antibacterial mechanism of the investigated complexes include the alteration of the permeability of the bacterial membrane. As a result, the tested complexes may leak through sugars and proteins to deactivate hydrogen respiratory chain enzymes, and subsequently, they produce pits and gaps in the bacterial membrane (peptidoglycan layer) to induce irregular fragmentation of the bacterial cells [54,55]. We therefore concluded that these indexes indicate that these complexes may lead to suitable biological functions.

**For (ID: 1VJY) transforming growth factor (TGF) for  $\beta$ -receptor type I ( $\beta$ -RI):** All complexes except five showed lower binding-score ( $\Delta G = -5.0$  Kcal/mol) than reference ligand460 ( $\Delta G = -4.81$  Kcal/mol), (Table S3, Supplementary Material). The six complexes showed significant binding-affinity ( $\Delta G = -4.13$  Kcal/mol). PLIF showed that the Leu.232 was bonded with 83.3% of complexes (2–6). Interestingly, the 1–6 complexes formed H-bond with amino acid backbone (Gly.212, Lys.232, Asp.281, and Ala.350) for  $\beta$ -RI (Figure S6, Supplementary Materials). The compounds interacted with important amino acids of  $\beta$ -RI binding-site as 1  $\rightarrow$  (Glu 254 and His.283), 2  $\rightarrow$  (Lys 232 and Sre280), 3  $\rightarrow$  Ala  $\rightarrow$  (230 and Lys 232); 4  $\rightarrow$  (Lys 232, Ser.280 and Ala.350), 5  $\rightarrow$  (Lys 232 and Val219), and 6  $\rightarrow$  (Lys 232 and Ser 280). The binding-affinity for 2–4 exhibited nearby equal  $\Delta G = \sim -2$  Kcal/mol.

### 3.9. Antimicrobial Tests

The prepared oxidovanadium (V) complexes were screened for antibacterial and antifungal activity and the obtained results are presented in Table 1. It is observed that the compounds are moderately active against both Gram-positive bacterial strains and the fungal strains, whereas all compounds were inactive against the Gram-negative bacterial strains. These observations suggest that the prepared vanadium mixed metal complexes had similar activity compared to our reported work earlier on vanadium complexes with triazole moiety [18,19]. It was reported that the biological activity of the used co-Ligands ( $L_2$ ,  $L_3$ , and  $L_4$ ) were moderate [56–58]. In our work it was observed the complexes with the co-ligand ( $L_4$ ) containing thiol group showed better activity than the other complexes. This may be due to the presence of two thiol groups which enhances the antimicrobial activity [19].

**Table 1.** Antimicrobial activity of the ligand (L1) and its vanadium (V) complexes.

Ligand and Complexes	“Antibacterial Activity 200 µg/disc”				“Antifungal Activity”
	“Gram-Positive Bacteria”		Gram-Negative Bacteria		Yeast
	<i>S.a</i>	<i>S.p</i>	<i>E.c</i>	<i>Pa</i>	<i>C.a</i>
NH <sub>4</sub> [VO(L <sub>1</sub> )(L <sub>2</sub> )] 2.5H <sub>2</sub> O(1)	0	20	0	0	12
K[VO(L <sub>1</sub> )(L <sub>2</sub> )] 1.5H <sub>2</sub> O (2)	12	23	0	0	17
NH <sub>4</sub> [VO(L <sub>1</sub> )(L <sub>3</sub> )] 4H <sub>2</sub> O(3)	12	26	7	6	11
K[VO(L <sub>1</sub> )(L <sub>3</sub> )] H <sub>2</sub> O (4)	16	21	0	0	14
NH <sub>4</sub> [VO(L <sub>1</sub> )(L <sub>4</sub> )] H <sub>2</sub> O (5)	0	24	0	0	13
K[VO(L <sub>1</sub> )(L <sub>4</sub> )]2 H <sub>2</sub> O (6)	15	21	9	7	18
<b>Amoxicillin</b>	28	35	21	23	0

S.a.: *Staphylococcus aureus* (ATCC 25923), S.p.: *Streptococcus pneumoniae* (ATCC 49619); E.c.: *Escherichia coli* (ATCC 25922); P.a.: *Pseudomonas aeruginosa* (ATCC 27853); C.a.: *Candida albicans* (ATCC 10231).

#### 4. Conclusions

The synthesized mixed-ligand oxidovanadium (V) complexes containing tri and bidentate ligands were of the general formulae NH<sub>4</sub>[VO(L<sub>1</sub>)(L<sub>2-4</sub>)]yH<sub>2</sub>O or K[VO(L<sub>1</sub>)(L<sub>2-4</sub>)]yH<sub>2</sub>O. The structures were proposed based on elemental analysis, mass spectra, IR, UV–visible, molar conductance, and <sup>1</sup>H NMR measurements. The synthesized mixed-ligand oxidovanadium (V) complexes were monomeric with octahedral geometry. The antimicrobial tests for the prepared compounds showed moderate activity against the Gram-positive bacteria type and fungal yeast.

**Supplementary Materials:** The following are available online at <https://www.mdpi.com/article/10.3390/pr9061008/s1>. Figure S1: IR spectrum for (1–6) complexes; Figure S2: The electronic spectrum of (1 and 4) complex; Figure S3: <sup>1</sup>H NMR spectrum of complexes (1–3); Figure S4: Mass spectra for (1, 3, 5, 6) complexes; Figure S5: optimization geometry of tested complexes (1–6) at DFT/PM6; Figure S6: Schematic interactions between ligands and proteins 4uro and 1VJY using protein–ligand interaction fingerprint tools; Table S1: The elemental analysis data and molar conductance measurements of the Vanadium (V) Complexes; Table S2: IR Spectroscopic data (cm<sup>-1</sup>) of the ligands and their vanadium (V) complexes; Table S3: Docking energy scores (kcal/mol) derived from the MOE for investigated complexes 1–6 and reference inhibitors Novobiocin & Naphthyridine.

**Author Contributions:** Conceptualization, M.A. and A.A.E.; methodology, M.A.; software, A.A.E.; validation, M.A., S.A.Z., and D.D.; formal analysis, M.A.; investigation, D.D.; resources, D.D.; data curation, M.A.; writing—original draft preparation, M.A. and D.D.; writing—review and editing, A.A.E.; visualization, M.A.; supervision, M.A. All authors have read and agreed to the published version of the manuscript.

**Funding:** This research received no external funding.

**Institutional Review Board Statement:** The study was conducted according to the guidelines of the Declaration of Albha university, and approved by the Institutional Review Board.

**Informed Consent Statement:** For studies not involving humans.

**Data Availability Statement:** Date of the compounds are available from the authors.

**Conflicts of Interest:** The authors declare no conflict of interest.

## References

1. Alaraji, Y.H.; Shneine, J.K.; Ahmed, A.N.A.A. Synthesis, characterization, and antibacterial activity of new Schiff's bases with 1,2,4-triazole moiety. *J. Sci.* **2015**, *5*, 293–299.
2. Al-Khuzai, M.G.; Al-Majidi, S.M. Synthesis, characterization and evaluation antimicrobial activity of some new substituted 2-mercapto-3-phenyl-4(3h)-quinazolinone. *Iraqi J. Sci.* **2014**, *55*, 582–593.
3. Akhter, M.W.; Hassan, M.Z.; Amir, M. Synthesis and pharmacological evaluation of 3-diphenylmethyl-6-substituted-1,2,4-triazolo[3,4-b]-1,3,4-thiadiazoles: A condensed bridgehead nitrogen heterocyclic system. *Arab. J. Chem.* **2014**, *7*, 955–963. [[CrossRef](#)]
4. Bekircan, O.; Menteş, E.; Ülker, S.; Kucuk, C. Synthesis of some new 1,2,4-triazole derivatives starting from 3-(4-chlorophenyl)-5-(4-methoxybenzyl)-4H-1,2,4-triazol with anti-lipase and anti-urease activities. *Arch. Pharm.* **2014**, *347*, 387–397. [[CrossRef](#)] [[PubMed](#)]
5. Aggarwal, R.; Sumran, G. An insight on medicinal attributes of 1,2,4-triazoles. *Eur. J. Med. Chem.* **2020**, *205*. [[CrossRef](#)]
6. Haasnoot, J.G. Mononuclear, oligonuclear and polynuclear metal coordination compounds with 1,2,4-triazole derivatives as ligands. *Coord. Chem. Rev.* **2000**, *200*, 131–185. [[CrossRef](#)]
7. Fang, Z.Y.; Zhang, L.; Ma, J.P.; Zhao, L.; Wang, S.L.; Xie, N.H.; Liu, Y.Q.; Guo, X.Y.; Qin, J. Dinuclear cobalt and nickel complexes of a mercaptoacetic acid substituted 1,2,4-triazole ligand: Syntheses, structures and urease inhibitory studies. *Acta Crystallogr. Sect. C Struct. Chem.* **2019**, *75*, 1658–1665. [[CrossRef](#)]
8. Althobiti, H.A.; Zabin, S.A. New Schiff bases of 2-(quinolin-8-yloxy)acetohydrazide and their Cu(ii), and Zn(ii) metal complexes: Their in vitro antimicrobial potentials and in silico physicochemical and pharmacokinetics properties. *Open Chem.* **2020**, *18*, 591–607. [[CrossRef](#)]
9. Sutradhar, M.; Fernandes, A.R.; Silva, J.; Mahmudov, K.T.; Da Silva, M.F.C.G.; Pombeiro, A.J. Water soluble heterometallic potassium-dioxidovanadium (V) complexes as potential antiproliferative agents. *J. Inorg. Biochem.* **2016**, *155*, 17–25. [[CrossRef](#)]
10. Levina, A.; Pires Vieira, A.; Wijetunga, A.; Kaur, R.; Koehn, J.T.; Crans, D.C.; Lay, P.A. A short-lived but highly cytotoxic vanadium (V) complex as a potential drug lead for brain cancer treatment by intratumoral injections. *Angew. Chem. Int. Ed.* **2020**, *59*, 15834–15838. [[CrossRef](#)]
11. De Lima, L.M.; Belian, M.F.; Silva, W.E.; Postal, K.; Kostenkova, K.; Crans, D.C.; Rossiter, A.K.F.; da Silva Júnior, V.A. Vanadium (IV)-diamine complex with hypoglycemic activity and a reduction in testicular atrophy. *J. Inorg. Biochem.* **2021**, *216*. [[CrossRef](#)]
12. Frank, P.; Carlson, R.M.K.; Carlson, E.J.; Hodgson, K.O. Medium-dependence of vanadium K-edge X-ray absorption spectra with application to blood cells from phlebobranch tunicates. *Coord. Chem. Rev.* **2003**, *237*, 31–39. [[CrossRef](#)]
13. Munawar, K.S.; Ali, S.; Tahir, M.N.; Khalid, N.; Abbas, Q.; Qureshi, I.Z.; Shahzadi, S. Investigation of derivatized Schiff base ligands of 1,2,4-triazole amine and their oxovanadium (IV) complexes: Synthesis, structure, DNA binding, alkaline phosphatase inhibition, biological screening, and insulin mimetic properties. *Russ. J. Gen. Chem.* **2015**, *85*, 2183–2197. [[CrossRef](#)]
14. Sutradhar, M.; Alegria, E.C.; Ferretti, F.; Raposo, L.R.; da Silva, M.F.C.G.; Baptista, P.V.; Fernandes, A.R.; Pombeiro, A.J. Antiproliferative activity of heterometallic sodium and potassiumdioxidovanadium (V) polymers. *J. Inorg. Biochem.* **2019**, *200*. [[CrossRef](#)]
15. Biswas, N.; Patra, D.; Mondal, B.; Drew, M.G.B.; Ghosh, T. Synthesis of mixed-ligand complexes of VO<sup>2+</sup> and VO<sup>3+</sup> incorporating hydrazone, 1,10-phenanthroline and 8-hydroxyquinoline. *J. Coord. Chem.* **2016**, *69*, 318–329. [[CrossRef](#)]
16. Sutradhar, M.; Pombeiro, A.J. Coordination chemistry of non-oxido, oxido and dioxidovanadium (IV/V) complexes with azine fragment ligands. *Coord. Chem. Rev.* **2014**, *265*, 89–124. [[CrossRef](#)]
17. Benítez, J.; Guggeri, L.; Tomaz, I.; Arrambide, G.; Navarro, M.; Pessoa, J.C.; Garat, B.; Gambino, D. Design of vanadium mixed-ligand complexes as potential anti-protozoa agents. *J. Inorg. Biochem.* **2009**, *103*, 609–616. [[CrossRef](#)] [[PubMed](#)]
18. Adeniyi, A.A.; Ajibade, P.A. Comparing the suitability of autodock, gold and glide for the docking and predicting the possible targets of Ru (II)-based complexes as anticancer agents. *Molecules* **2013**, *18*, 3760–3778. [[CrossRef](#)] [[PubMed](#)]
19. Alikhani, M.; Hakimi, M.; Moeini, K.; Mashreghi, M.; Eigner, V.; Dusek, M. Spectral, structural, biological and molecular docking studies of a new mixed-valence V (IV)/V (V) ofloxacin complex. *J. Mol. Struct.* **2020**, *1216*. [[CrossRef](#)]
20. Gómez, V.; Benet-Buchholz, J.; Martin, E.; Galán-Mascarós, J.R. Hysteretic spin crossover above room temperature and magnetic coupling in trinuclear transition-metal complexes with anionic 1,2,4-triazole ligands. *Chem. A Eur. J.* **2014**, *20*, 5369–5379. [[CrossRef](#)]
21. Sumra, S.H.; Anees, M.; Asif, A.; Zafar, M.N.; Mahmood, K.; Nazar, M.F.; Khalid, M.; Nadeem, M.A.; Khan, M.U. Synthesis, structural, spectral and biological evaluation of metals endowed 1,2,4-Triazole. *Bull. Chem. Soc. Ethiop.* **2020**, *34*, 335–351. [[CrossRef](#)]
22. Sener, S.; Kul, I.; Bhat, K. Photochemical reactions of metal carbonyls [M(CO)<sub>6</sub> (M = Cr, Mo, W), Mn(CO)<sub>3</sub> Cp] with 4-amino-3-hydrazino-5-mercapto-1,2,4-triazole (AHMT) and 3-amino-5-mercapto-1,2,4-triazole (AMT). *Synth. React. Inorg. Met. Nano-Met. Chem.* **2015**, *45*, 495–501. [[CrossRef](#)]
23. Sanoja, W.; Martínez, J.D.; Araujo, M.L.; Brito, F.; Hernández, L.; Del Carpio, E.; Lubes, V. Stability constants of mixed ligand complexes of vanadium (III) with 8-hydroxyquinoline and the amino acids glycine, proline, α-alanine and β-alanine. *J. Mol. Liq.* **2014**, *197*, 223–225. [[CrossRef](#)]
24. Dales, G.E.; Kostrewa, D.; Gsell, B.; Stieger, M.; D'Arcy, A. Crystal engineering: Deletion mutagenesis of the 24 kDa fragment of the DNA gyrase B subunit from *Staphylococcus aureus*. *Acta Crystallogr. Sect. D Biol. Crystallogr.* **1999**, *55*, 1626–1629. [[CrossRef](#)]

25. Gellibert, F.; Woolven, J.; Fouchet, M.-H.; Mathews, N.; Goodland, H.; Lovegrove, V.; Laroze, A.; Nguyen, V.-L.; Sautet, S.; Wang, R.; et al. Identification of 1,5-naphthyridine derivatives as a novel series of potent and selective TGF- $\beta$  type I receptor inhibitors. *J. Med. Chem.* **2004**, *47*, 4494–4506. [[CrossRef](#)]
26. Rana, R.; Sharma, R.; Kumar, A. Repurposing of fluvastatin against *Candida albicans* CYP450 lanosterol 14  $\alpha$ -demethylase, a target enzyme for antifungal therapy: An in silico and in vitro study. *Curr. Mol. Med.* **2019**, *19*, 506–524. [[CrossRef](#)]
27. Jacob, K.S.; Ganguly, S.; Kumar, P.; Poddar, R.; Kumar, A. Homology model, molecular dynamics simulation and novel pyrazole analogs design of *Candida albicans* CYP450 lanosterol 14  $\alpha$ -demethylase, a target enzyme for antifungal therapy. *J. Biomol. Struct. Dyn.* **2017**, *35*, 1446–1463. [[CrossRef](#)]
28. Kant, K.; Lal, U.R.; Kumar, A.; Ghosh, M. A merged molecular docking, ADME-T and dynamics approaches towards the genus of Arisaema as herpes simplex virus type 1 and type 2 inhibitors. *Comput. Biol. Chem.* **2019**, *78*, 217–226. [[CrossRef](#)]
29. Navyashree, V.; Kant, K.; Kumar, A. Natural chemical entities from Arisaema genus might be a promising break-through against Japanese encephalitis virus infection: A molecular docking and dynamics approach. *J. Biomol. Struct. Dyn.* **2020**, 1–13. [[CrossRef](#)] [[PubMed](#)]
30. Gupta, M.; Sharma, R.; Kumar, A. Comparative potential of simvastatin, rosuvastatin and fluvastatin against bacterial infection: An in silico and in vitro study. *Orient. Pharm. Exp. Med.* **2019**, *19*, 259–275. [[CrossRef](#)]
31. Frisch, M.J.; Schlegel, H.B.; Scuseria, G.E.; Robb, M.A.; Cheeseman, J.R.; Scalmani, G.; Barone, V.; Mennucci, B.; Petersson, G.A.; Nakatsuji, H.; et al. *Gaussian 09, Revision*; Gaussian, Inc.: Wallingford, CT, USA, 2013.
32. Chemical Computing Group ULC. *Molecular Operating Environment (MOE) 1010 Handbook*; Chemical Computing Group ULC: Montreal, QC, Canada, 2017.
33. Laurie, A.T.R.; Jackson, R.M. Q-SiteFinder: An energy-based method for the prediction of protein–ligand binding sites. *Bioinformatics* **2005**, *21*, 1908–1916. [[CrossRef](#)]
34. Zabin, S.A.; Abdelbaset, M. Oxo/dioxo-vanadium (V) complexes with Schiff base ligands derived from 4-amino-5-mercapto-3-phenyl-1,2,4-triazole. *Eur. J. Chem.* **2016**, *7*, 322–328. [[CrossRef](#)]
35. Yaul, A.; Pethe, G.; Deshmukh, R.; Aswar, A. Vanadium complexes with quadridentate Schiff bases: Synthesis, characterization, thermal and catalytic studies. *J. Therm. Anal. Calorim.* **2013**, *113*, 745–752. [[CrossRef](#)]
36. Kareem, A.; Khan, M.S.; Nami, S.A.A.; Bhat, S.A.; Mirza, A.U.; Nishat, N. Curcumin derived Schiff base ligand and their transition metal complexes: Synthesis, spectral characterization, catalytic potential and biological activity. *J. Mol. Struct.* **2018**, *1167*, 261–273. [[CrossRef](#)]
37. Singh, K.; Kumar, Y.; Puri, P.; Singh, G. Spectroscopic, thermal, and antimicrobial studies of Co(II), Ni(II), Cu(II), and Zn(II) complexes derived from bidentate ligands containing N and S donor atoms. *Bioinorg. Chem. Appl.* **2012**, *2012*, 1–9. [[CrossRef](#)] [[PubMed](#)]
38. Kulkarni, N.V.; Sathisha, M.P.; Budagumpi, S.; Kurdekar, G.S.; Revankar, V.K. Binuclear transition metal complexes of bi-compartmental SNO donor ligands: Synthesis, characterization, and electrochemistry. *J. Coord. Chem.* **2010**, *63*, 1451–1461. [[CrossRef](#)]
39. Abdelbaset, M.; Zabin, S. Vanadium (V) complexes containing 1,2,4-triazole moiety and their antimicrobial activity. *Int. J. Adv. Res.* **2016**, *4*, 1861–1871. [[CrossRef](#)]
40. Barakat, A.S.; Gaballa, A.S.; Mohammed, S.F.; Teleb, S.M. Vibrational and thermal studies of the complexes (NH<sub>4</sub>)[VO(O<sub>2</sub>)<sub>2</sub>(phen)]·2H<sub>2</sub>O and (NH<sub>4</sub>)[V(O<sub>2</sub>)<sub>3</sub>(phen)]·2H<sub>2</sub>O. *Spectrochim. Acta Part. A Mol. Biomol. Spectrosc.* **2005**, *62*, 814–818. [[CrossRef](#)] [[PubMed](#)]
41. Alghamdi, I.A.; Abdelbaset, M.; El Mannoubi, I. Mixed ligand complexes of copper(II) and cobalt(II) with hydrazones derivatives and ortho-vanillin: Syntheses, characterizations and antimicrobial activity. *Orient. J. Chem.* **2019**, *35*, 1722–1730. [[CrossRef](#)]
42. Thakur, S.; Sarkar, N.; Drew, M.G.B.; Bauzá, A.; Frontera, A.; Chattopadhyay, S. Estimating the energy of noncovalent interactions in a dioxovanadium (V) Schiff base complex: Exploration of its phenoxazinone synthase like activity. *Polyhedron* **2018**, *142*, 83–92. [[CrossRef](#)]
43. Maurya, R.C.; Rajput, S. Neutral dioxovanadium (V) complexes of biomimetic hydrazones ONO donor ligands of bioinorganic and medicinal relevance: Synthesis via air oxidation of bis(acetylaceto-nato)oxovanadium (IV), characterization, biological activity and 3D molecular modeling. *J. Mol. Struct.* **2007**, 833. [[CrossRef](#)]
44. Zabin, S.A.; Abdelbaset, M. Vanadium (V) complexes containing 1,2,4-triazole moiety and their antimicrobial activity. *Eur. J. Chem.* **2016**, *7*, 322–328. [[CrossRef](#)]
45. Singh, K.; Singh, D.P.; Singh Barwa, M.; Tyagi, P.; Mirza, Y. Some bivalent metal complexes of Schiff bases containing N and S donor atoms. *J. Enzym. Inhib. Med. Chem.* **2006**, *21*, 749–755. [[CrossRef](#)]
46. Haddad, R.; Yousif, E.; Ahmed, A. Synthesis and characterization of transition metal complexes of 4-Amino-5-pyridyl-4H-1,2,4-triazole-3-thiol. *Springerplus* **2013**, *2*, 510. [[CrossRef](#)]
47. Kumaran, J.S.; Priya, S.; Jayachandramani, N.; Mahalakshmi, S. Synthesis, spectroscopic characterization and biological activities of transition metal complexes derived from a tridentate schiff base. *J. Chem.* **2013**. [[CrossRef](#)]
48. Wildman, S.A.; Crippen, G.M. Prediction of physicochemical parameters by atomic contributions. *J. Chem. Inf. Comput. Sci.* **1999**, *39*, 868–873. [[CrossRef](#)]
49. Al-Harbi, L.M.; Nassar, H.S.; Moustfa, A.; Alosaimi, A.M.; Mohamed, H.M.; Khowdiary, M.M.; El-Gazzar, M.A.; Elhenawy, A.A. Novel coumarin amino acid derivatives: Design, synthesis, docking, absorption, distribution, metabolism, elimination, toxicity (admet), quantitative structure–activity relationship (qsar) and anticancer studies. *Mater. Express* **2020**, *10*, 1375–1394. [[CrossRef](#)]

50. Aldred, K.J.; McPherson, S.A.; Turnbough, C.L.; Kerns, R.J.; Osheroff, N. Topoisomerase IV-quinolone interactions are mediated through a water-metal ion bridge: Mechanistic basis of quinolone resistance. *Nucleic Acids Res.* **2013**, *41*, 4628–4639. [[CrossRef](#)]
51. Jung, W.K.; Koo, H.C.; Kim, K.W.; Shin, S.; Kim, S.H.; Park, Y.H. Antibacterial activity and mechanism of action of the silver ion in *Staphylococcus aureus* and *Escherichia coli*. *Appl. Environ. Microbiol.* **2008**, *74*, 2171–2178. [[CrossRef](#)]
52. Corbeil, C.R.; Williams, C.I.; Labute, P. Variability in docking success rates due to dataset preparation. *J. Comput. Mol. Des.* **2012**, *26*, 775–786. [[CrossRef](#)]
53. Amro, N.A.; Kotra, L.P.; Wadu-Mesthrige, K.; Bulychev, A.; Mobashery, S.; Liu, G.Y. High-resolution atomic force microscopy studies of the *Escherichia coli* outer membrane: Structural basis for permeability. *Langmuir* **2000**, *16*, 2789–2796. [[CrossRef](#)]
54. Pellieux, C.; Dewilde, A.; Pierlot, C.; Aubry, J.M. Bactericidal and virucidal activities of singlet oxygen generated by thermolysis of naphthalene endoperoxides. *Methods Enzymol.* **2000**, *319*, 197–207. [[CrossRef](#)]
55. Feng, Q.L.; Wu, J.; Chen, G.Q.; Cui, F.Z.; Kim, T.N.; Kim, J.O. A mechanistic study of the antibacterial effect of silver ions on *Escherichia coli* and *Staphylococcus aureus*. *J. Biomed. Mater. Res.* **2000**, *52*, 662–668. [[CrossRef](#)]
56. Mahmoud, W.H.; Deghadi, R.G.; Mohamed, G.G. Metal complexes of novel Schiff base derived from iron sandwiched organometallic and 4-nitro-1,2-phenylenediamine: Synthesis, characterization, DFT studies, antimicrobial activities and molecular docking. *Appl. Organometal. Chem.* **2018**, *32*, e4289. [[CrossRef](#)]
57. Aziz, A.A.A.; Salem, A.N.M.; Sayed, M.A.; Aboaly, M.M. Synthesis, structural characterization, thermal studies, catalytic efficiency and antimicrobial activity of some M(II) complexes with ONO tridentate Schiff base N-salicylidene-o-aminophenol (saphH2). *J. Mol. Struct.* **2012**, *1010*, 130–138. [[CrossRef](#)]
58. Bharti, S.; Choudhary, M.; Mohan, B.; Rawat, S.P.; Sharma, S.R.; Ahmad, K. Syntheses, spectroscopic characterization, SOD-like properties and antibacterial activities of dimer copper (II) and nickel (II) complexes based on imine ligands containing 2-aminothiophenol moiety: X-ray crystal structure determination of disulfide Schiff bases. *J. Mol. Struct.* **2018**, *1164*, 137–154.